Energy Advances

ROYAL SOCIETY OF CHEMISTRY

PAPER

View Article Online
View Journal | View Issue

Cite this: *Energy Adv.*, 2024, 3, 2407

Feasibility study of UV intensity monitoring in water disinfection systems using reverse-biased LED photometers†

D. Pousty, *‡ Y. Gerchman‡ and H. Mamane

Common ultraviolet (UV) photodiodes or detectors for measuring the intensity of UV-light-emitting diodes (LEDs) in UV disinfection systems are costly. This study explores the potential of using low-cost UV-LEDs as photometers for monitoring UV intensity in water systems. Reverse LEDs (rLEDs) generate a small current proportional to the incident light intensity on the p–n junction when operated in unbiased mode. rLEDs with different wavelengths and power levels were examined to find the optimal rLED for monitoring the intensity of a 275 nm LED strip, achieving less than 1% deviation from a calibrated spectroradiometer. The influence of temperature was also examined on rLED measurements and found non-negligible. This work demonstrates the feasibility of using rLEDs as intensity monitoring sensors for UV-C LED sources, offering a low-cost and reliable alternative for UV intensity monitoring in UV-LED water disinfection systems.

Received 16th November 2023,
Accepted 1st August 2024

DOI: 10.1039/d3ya00554b

rsc.li/energy-advances

1. Introduction

The World Health Organization (WHO) reported in March 2021 that over 2 billion people globally still lack safe water services.[1] Resolving this issue necessitates substantial efforts to scale up and extend the water supply to individual households and implement strategies for treating contaminated water at its source. In these settings, it is essential that water treatment technologies are durable and robust, minimizing the requirement for frequent and expensive maintenance. These technologies should also be easy to operate, independent of external inputs, and affordable.[2]

Ultraviolet (UV) light-based water disinfection technology is used for the inactivation of pathogens in both drinking water and wastewater effluents.[3] Low-pressure (LP) UV-mercury vapor lamps are the most prevalent UV-based point-of-use (POU) systems with several significant drawbacks; despite their effectiveness.[4] These lamps are fragile, lack adaptability for smaller-scale systems, and contain toxic mercury, thus necessitating the availability of disposal facilities. LP lamps are monochromatic in nature and, thus, less effective in preventing the recovery of microorganisms post UV, compared to polychromatic medium-pressure (MP) lamps.[5] Additionally, these lamps consume substantial energy due to their low wall plug efficiency, which ranges from approximately 15% to 35%, and they have a relatively short lifespan of less than 10 000 hours.[4,6]

UV light-emitting diodes (LEDs) are emerging as a POU UV-based technology for water disinfection; UV-LEDs are compact and have low energy consumption compared to other light source technologies such as mercury and excimer lamps.[7] This characteristic allows using solar panels[8,9] and innovative design architecture for UV disinfection systems based on LED technology for point-of-use systems.[9–11] UV-LEDs are characterized by a gradual degradation in radiation intensity over their operational lifetime (more than 10 000 hours,[12]), avoiding catastrophic failures.[13,14] UV-LEDs have the capability to emit light at specific wavelengths, allowing a flexible tailored design for POU UV-based systems that can combine selected wavelengths for optimal inactivation of different pathogens.[15]

Currently, the determination of UV intensity primarily relies on the use of spectroradiometers or radiometers, which, despite their accuracy, come with significant drawbacks: they are notably expensive, fragile, and require skilled personnel for operation, thus limiting their suitability for remote areas.[16] Moreover, the design and dimensions of these probes do not accommodate the measurement of UV intensity in real UV-LED flow-through systems, where varied geometries and flow conditions significantly complicate the process. Alternatively, chemical actinometers (*e.g.*, ferrioxalate, iodide–iodate, nitrate, uridine) offer a method to determine UV light intensity across different sources, given their known quantum yields.[17–20] Each actinometer requires specific conditions for optimal use, along with distinct protocols for

School of Mechanical Engineering, Faculty of Engineering, Tel Aviv University, Tel Aviv 69978, Israel. E-mail: danapousty@mail.tau.ac.il, hadasmg@tauex.tau.ac.il, ygerchman@gmail.com

† Electronic supplementary information (ESI) available. See DOI: https://doi.org/10.1039/d3ya00554b

‡ These authors contributed equally to this work.

operation. While this approach is adaptable and reliable, it necessitates laboratory execution under controlled conditions, such as a dark room or specific temperatures, thus precluding its use in field settings.[16,21,22]

Despite the potential of UV-LED technology in water disinfection, the lack of affordable and reliable UV intensity monitoring systems remains a significant challenge. Linden *et al.*[23] highlighted the necessity for robust monitoring solutions that can operate effectively in diverse environmental conditions, particularly in low-income regions where access to safe water is critically needed. The need for low-cost UV sensors is further emphasized by the work of Chatterley and Linden (2010),[4] who explored the demonstration and evaluation of germicidal UV-LEDs for point-of-use water disinfection, identifying the gap in affordable monitoring technologies. Thus, there is a need to develop a low-cost UV LED sensor that can be integrated into water disinfection systems in rural and low-income settings.

One interesting UV sensor called a paired emitter detector diode (PEDD) relies on the electroluminescence effect in direct bandgap semiconductors that act in a reverse mode. UV-vis LEDs operate based on the electroluminescence effect in direct bandgap semiconductor materials[24,25] and their emission spectrum is determined by the materials it is made of and the junction temperature.[26] The UV-vis LED is considered one of the critical components in optoelectronic devices due to the multitude of factors that drive its development.[25,27] The most important ones are brightness, efficiency, flexibility, lifetime, durable construction, low power consumption, and suitable operating voltage.[28]

Based on the PEDD concept, a simple UV LED can be used in a reversal mode as a photometer, termed in this study reverse LED (rLED). When light with sufficient energy is irradiated upon the LED's p–n junction, a small current is produced, proportional to the light intensity. This photocurrent can be measured and therefore, the source intensity can be determined. Pioneering studies in the 1970s formed the basis for LED-based optical absorption detectors (LED-based photometers).[26,29] O'Toole *et al.* developed a paired emitter detector-diode (PEDD) flow cell[30–32] and applied this device as a detector in liquid chromatography.[33,34] Lau *et al.* also developed a multi-LED photometer as an alternative reflectance-based optical sensor configuration.[35] This sensor employs an array of LEDs as light sources (40–880 nm), which surrounds a central detector LED (940 nm). This approach facilitated the analysis of multiple dyes both separately and in mixtures. Lange *et al.* (2011) demonstrated the use of multicolor LEDs in luminescence sensing applications for environmental properties like temperature and pressure, highlighting their effectiveness as both excitation sources and detectors due to their wavelength selectivity and sensitivity.[36]

LED-based sensors offer greater accuracy and are much more cost-effective than conventional devices.[37] LED-based detectors can detect light with wavelengths equal to or shorter than their spectral emission band, as electrons undergo band transition to generate a photocurrent. LED application as an intensity sensor for the visible range is well known,[38] with low power consumption, and can respond to a broad spectral range (247 nm to >900 nm). However, the generated photocurrent is extremely small, typically in the picoampere range. This poses a significant challenge in measuring such low currents with simple devices, as highly sensitive current meters tend to be expensive and bulky in size.

To address this gap, the current research concept was inspired by publications from Dermot Diamond's group.[30,39] The rLED photometer operates by applying a reverse bias to the p–n junction for a sufficient duration, allowing it to function as a capacitor. When the external reverse bias is removed, the photocurrent generated by the incident light discharges the capacitance of the junction. During this time, a voltage meter measures the potential of the junction. The light intensity can be directly determined by measuring the time taken for this discharge process through a simple circuit. Moreover, the intensity of LEDs is strongly influenced by temperature.[40] Experiments showed a negative correlation between LED intensity and temperature. Various theoretical models have been developed to estimate this temperature-dependent behavior. When utilizing rLEDs as photometers, it is crucial to account for the thermal effects on measurements and implement appropriate compensation techniques if the impact is significant.

An extensive review of UV light detection solutions, including conventional sensor alternatives, is illustrated in a tree diagram showing diverse approaches for monitoring UV intensity, both as an integral part of a system and as a standalone device (ESI,† Fig. S1). This research aims to determine the performance of rLEDs in UV-LED disinfection systems and the sensitivity of rLED measurements to temperature variations, while evaluating the potential accuracy and reliability of these measurements.

2. Materials and methods

2.1 UV LED source

Twelve UV LED diodes (Violumas VC12X1C48LB-275 series), emitting light at a wavelength of 275 nm, were coupled with a heat sink (VC12X1) to ensure balanced heat distribution across the LED strip. The UV spectra of the UV-LED strip were measured using an Ocean Optics USB4000 spectroradiometer equipped with a cosine corrector (OCF-104447, EOS-A1241604). The strip UV LEDs exhibited peak wavelength emissions at 267.2 nm with FWHM bandwidths of 13.5 nm. The UV source was controlled by an analog dimming unit that employed a resistor to manage the input current, allowing for the adjustment of the light source power within the range of 0 to 34 Watts. Five working points were examined, covering a broad power range of 9 W, 15 W, 21 W, 27 W, and 33 W (ESI,† Fig. S2). To reduce the incident irradiance, a neutral density (ND) filter (FDU-0.4, OFR, NJ, USA) was used with UV-C region transmission of ~40%. The transmission curves for the ND filters were measured with a spectrophotometer (V1100D, MRC Ltd, Holon, Israel) equipped with an integrating sphere attachment (diffuse reflectance accessory [DRA]-CA-3330, Labsphere) to confirm no change in the spectrum (ESI,† Fig. S3).

2.2 rLED

Five types of rLEDs were examined, each type featuring two independent LEDs, with identical emission parameters. These

Table 1 rLEDs list and characteristics

1st rLED ID	2nd rLED ID	Peak wavelength [nm]	Power [W]	Forward current [mA]	Forward voltage [V]	FWHM [nm]
L1	L7	310	1	100	6	10
L2	L8	365	1	300	3.5	10
L3	L9	405	3	600	3.5	14
L4	L10	365	3	600	3.5	9
L5	L6	365	10	1300	6.9	13

rLEDs are commercially available products from the "UVTaoYuan" company. A detailed list of LEDs and their characteristics is presented in Table 1.

2.3 Experiment set-up

Fig. 1 illustrates a schematic diagram of the system setup. In brief, the UV LED strip is positioned horizontally with its face-down orientation on an aluminum stand (Fig. S4, ESI† presents a photo of the study setup). Directly beneath the center of the UV strip, the photometers were placed (spectroradiometer or rLED). The distance between the UV-LED source and the sensor front plane was 17.5 cm and 11.5 cm for rLEDs and the spectroradiometer (Ocean Optics USB4000), respectively, constrained by the sensor's geometry. The neutral density filter was placed horizontally on the optical path to reduce irradiance density to avoid invalid saturated values caused by optical dazzling. The rLED sensor was electrically connected to an Arduino Nano developing board (ESI,† Fig. S5) and then linked to a monitor display. All the experiments were conducted with the same configuration and set up and conditions.

2.4 Experiment design

The feasibility of using rLED photometers as a UV intensity monitor was tested for rLED parameters (wavelength and forward power) and the rLED temperature. To test the influence of the rLED parameters, five types of rLEDs were tested (as mentioned in Section 1.2). For measuring the external temperature influence on rLED measurements, a 365 nm/3 W rLED contact has been capsulated with a domestic heat melting glue and the whole rLED was placed in a small water bath to avoid condensation effects on the rLED lens due to temperature differences. Two temperature sensors were applied to the device (ESI,† Fig. S6), one was attached to the rLED backside and the other monitored the environment to avoid source intensity errors due to thermal changes. The water temperature changed in the range of 5 °C to 40 °C, while the light source was kept at a constant intensity.

2.5 Data analysis

Following the introduction, the Arduino board collects the values of time taken to the rLEDs getting discharged between two potential levels (4.5 V and 1.5 V) during 100 re-biasing cycles (typically in the range of hundreds of milliseconds) (program code can be found on ESI,† Appendix S1). The time taken for the discharging process of the rLED should decay exponentially, so in order to get a sensible result, the output of the calculation is the multiplicative inverse of averaged time.

These values vary depending on the system configuration, geometry, and components; therefore, they should be considered relatively.

The measured data was analyzed using SAS JMP 17 statistical software including all calculations and statistical tests. In a box plot format, the middle bar represents the median, the "*x*" sign indicates the average values and the box contains 50%

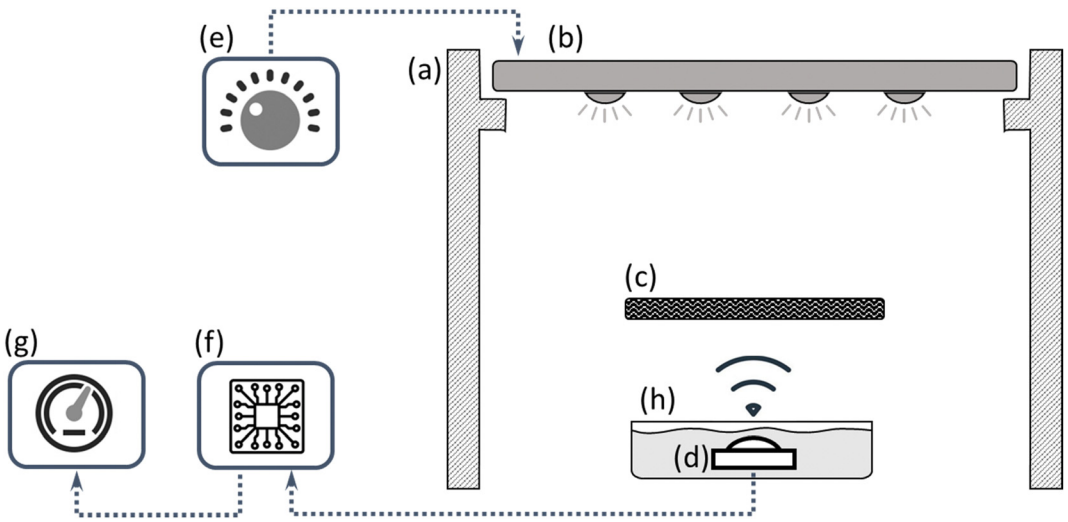

Fig. 1 Test configuration schematic diagram. (a) Light source stand; (b) light strip source; (c) neutral density filter; (d) rLED sensor or spectroradiometer; (e) light control unit; (f) Arduino developing board; (g) display monitor; (h) temperature-controlled bath, applied only for the thermal dependency test.

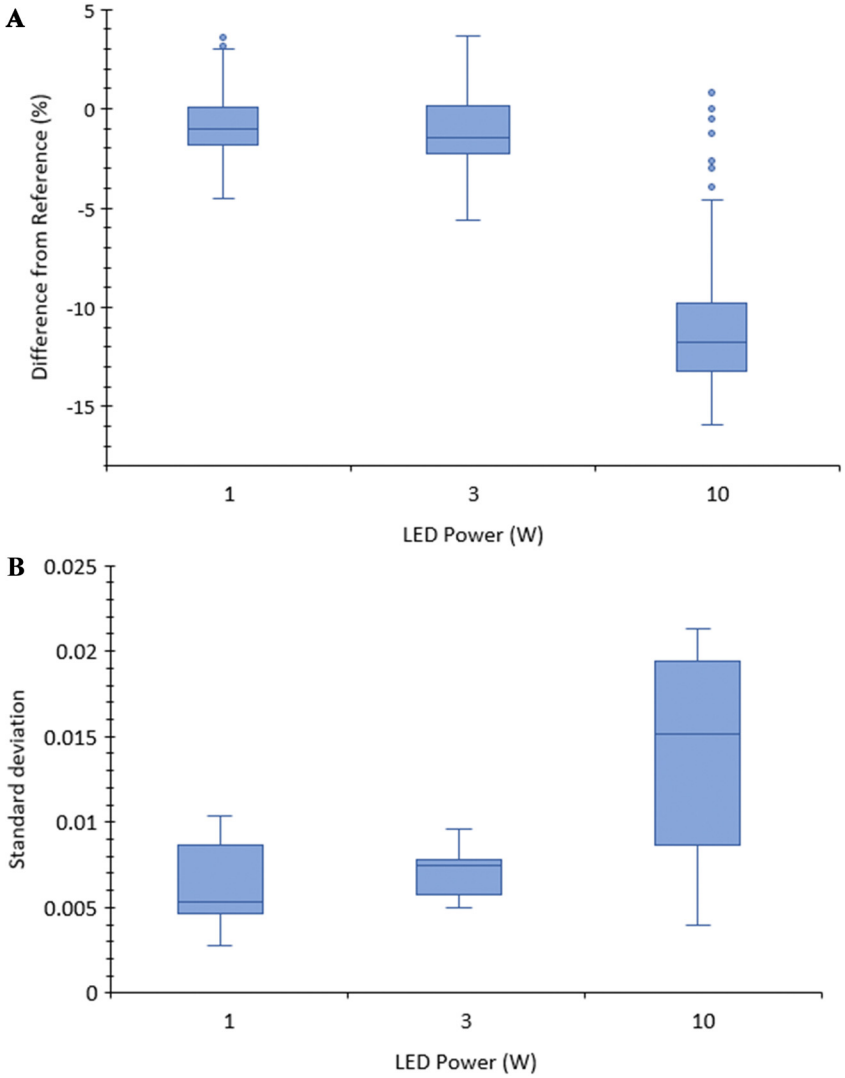

Fig. 2 (A) Comparison between 365 nm rLED power differences from reference. (B) Comparison between rLED power standard deviation.

of all data points, with the box edges representing the high and low quartiles (as presented in Fig. 2 and 3). IQR corresponds to the length of the box in the box plot and is used to define the length of the graph's whiskers. The whiskers (the two thin bars) present the closest data point, which can be found in the range of 1.5 × IQR from the closest box edge. Data points that fell out of the boxplot amplitude were suspicious as outliers and drawn as a single point.

2.6 Statistical analysis

All pairwise comparisons among group means were performed using the Tukey–Kramer test to determine significant differences between datasets, using JMP statistic software. All statistical analyses were conducted at a 95% confidence level using JMP statistic software. Error bars correspond to the 95% confidence interval on the mean unless otherwise noted. The correlation between source power and rLED output can be found in ESI,† Fig. S7.

3. Results and discussion

3.1 Influence of rLED properties

This study examined the use of reverse LEDs as UV-LED intensity detectors. All five source power working points (using all ten rLEDs as outlined in Table 1) were measured and analyzed to examine if rLED readings align with the values obtained from the calibrated spectroradiometer. This data was subsequently normalized to the maximum values within their respective groups and then compared to the calibrated spectroradiometer, which was also normalized to its maximum value, designated as the reference value. Table S4, ESI,† presents a summary of the results. Fig. 2 illustrates the comparison between rLED power, expressed as percentage differences from the reference values, and the standard deviation of the measurements, which indicates the measurement noise level.

1 W rLED was tested and compared for illuminated and unilluminated modes. The differences showed significant and allowed unilluminated signal filtration, for the unilluminated

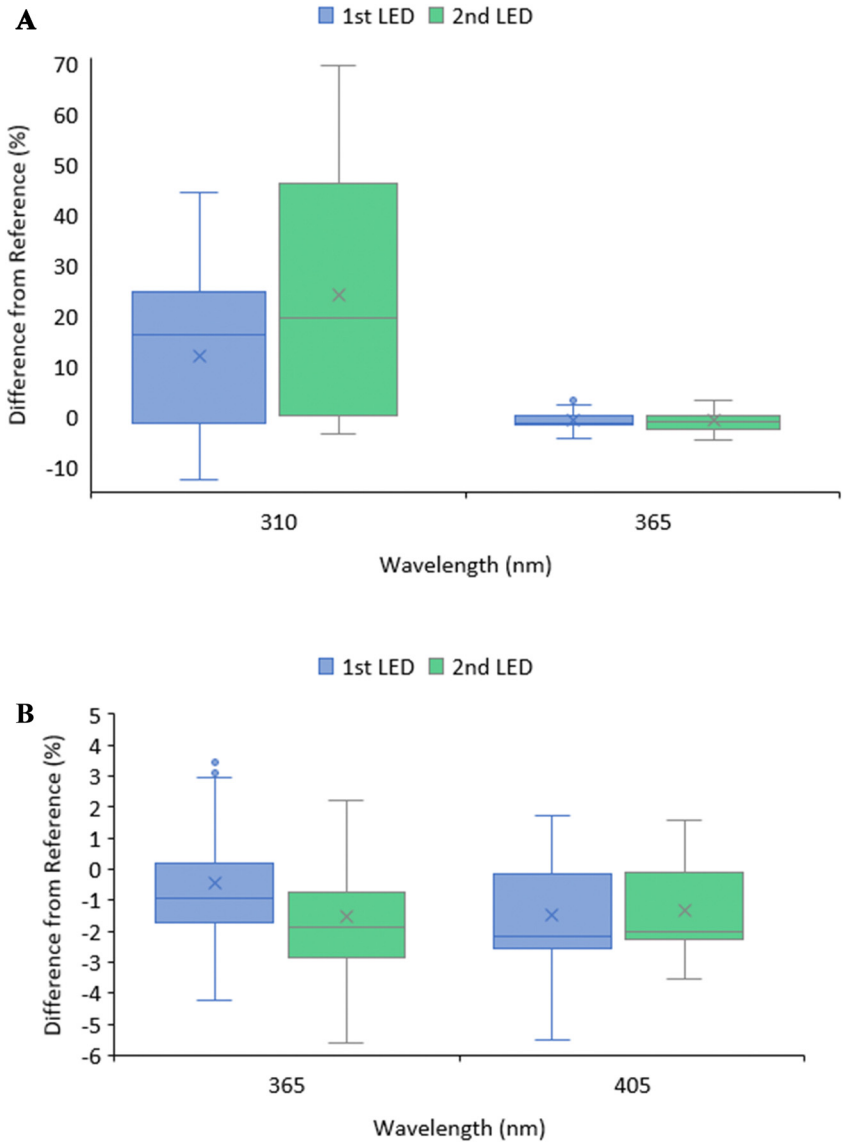

Fig. 3 (A) Comparison between rLED wavelength −1 W. (B) Comparison between rLED wavelength −3 W.

case where the discharging process took a few hours and for the illuminated case it took less than 1.5 s. The 1 W setting exhibits the best performance, with a difference from the reference measurements of less than 1% for the median and a relatively small standard deviation.

The 3 W setting performs similarly, with the median difference from the reference being less than 1.5%. The Tukey–Kramer statistical tests show a significant difference between these two rLEDs, with a p-value < 0.02. The 10 W rLED produced notably inferior results, with an approximate 12% difference from the reference and a higher standard deviation. Its Tukey–Kramer p-value is < 0.001, signifying a highly significant statistical difference compared to the reference.

This discrepancy may be attributed to geometry differences between 10 W and the 1 W and 3 W LEDs. It is essential to consider the differences in design when comparing the influence of rLED power. The 1 W and 3 W models share the same geometry, while the 10 W model differs slightly, featuring a larger (double) cover transparent lens and being attached to a copper heat sink instead of aluminum. These design disparities may have an impact on the observed performance variations.

Fig. 3 presents a comparison of two distinct splits, with each split comprising rLEDs that share similar forward power levels. This comparison allows us to find the influence of the wavelength with constant rLED power. The deviations from the reference were compared between 310 nm and 365 nm for the 1 W rLEDs and between 365 nm and 405 nm for the 3 W rLEDs.

When transitioning from the 310 nm rLED to the 365 nm rLED, the difference from the reference shifts from 18% to approximately −1%. Similarly, for the 3 W rLEDs, there is a similar trend, but with a much smaller magnitude. The 365 nm rLED exhibits a −1% difference from the reference, while the 405 nm rLED shows approximately −1.4%. These results show that maintaining a significant frequency gap between the rLED

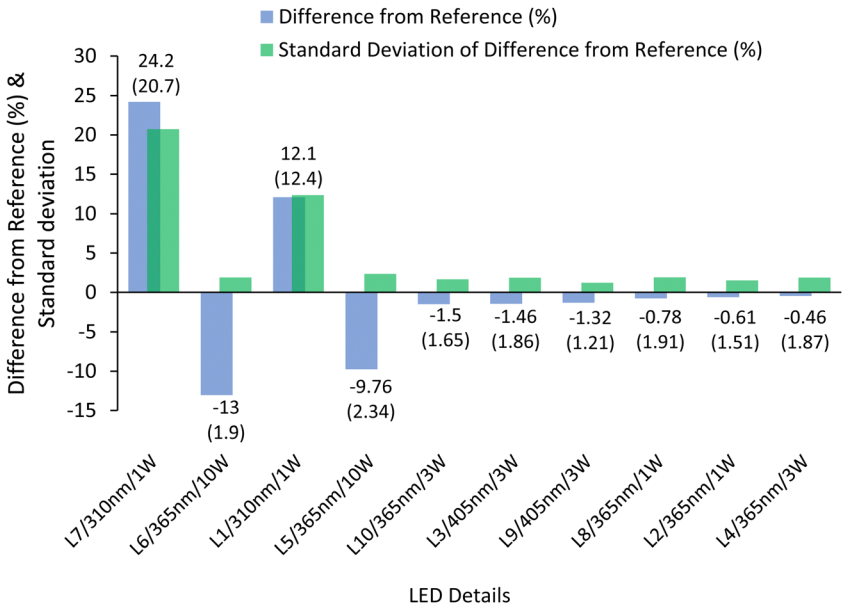

Fig. 4 rLED cross comparison.

and the monitored source is crucial. For instance, using an rLED with a frequency approximately 33% lower than that of the source has been employed to achieve satisfactory results. This suggests that carefully selecting the rLED wavelength relative to the source is essential for accurate measurements. The summary of the two previous comparisons is illustrated in Fig. 4, with the data ordered based on the absolute difference from the reference values. All rLEDs, specifically those with wavelengths longer than 310 nm and lower forward power than 10 W, produce accuracy results of less than 1.5% absolute difference from the reference and relatively small standard deviations.

A cross-analysis taking into account both the rLED wavelength and power, while considering the need for a lower absolute difference from the reference and a preference for lower standard deviations, suggests that the optimal working point is with the 365 nm/3 W rLED. However, it is essential to recognize that this choice is based solely on the information gathered from the current experiments and may shift if additional types of rLEDs are tested. The long-term stability of the 365 nm/3 W rLED used as a detector under UVC irradiation was tested (under the same setup and conditions of previous experiments); the sample was taken every 3 hours, for 240 hours (Fig. S8, ESI†). The graph depicts the normalized light intensity (normalized for the highest intensity measured) over a period of 240 hours. Initially, there is an increase in the source power until the maximum power is reached, followed by a stabilization phase. The deviations during this stabilization phase are less than 0.5%, indicating a high level of consistency between measurements. During the rise phase, the deviation between the maximum and minimum power is less than 4%, which falls within an acceptable range of variability. Overall, the data demonstrates stability throughout the entire measurement period, confirming the reliability of the UV intensity monitoring system.

The study conducted by Dasgupta *et al.* 1993[26] examined visible LEDs with wavelengths of 555, 570, 605, and 660 nm, both as detectors and emitters. Their findings indicated that the LED with a wavelength of 660 nm exhibited the best performance as a detector when measuring photocurrent. The conclusions drawn from this study were two-fold. It was established that LEDs can be employed as dual-wavelength detectors, and the study suggested that this approach is not practical. However, with the advancement of LED technology, LEDs have become a reliable source for various applications, including their use as detectors. Toole *et al.* 2005[30] controlled the emitter LED emission intensity using a variable resistor. Therefore, an increase in the resistance resulted in a decrease in the light intensity of the emitter LED, which in turn resulted in an increase in the time taken to discharge the detector LED. They showed that increasing the resistance by 2 kΩ improved the sensitivity by an approximate factor of 4. Toole *et al.* (2006) utilized a timer circuit to measure the time taken for the photocurrent generated by the emitter LED (λ_{max} 500 nm) to discharge the detector LED (λ_{max} 621 nm), rather than measuring the photocurrent directly.[30] LEDs can detect light with wavelengths shorter than their emission band due to the band transition of electrons generating a photocurrent. This inherent property of LEDs supports the claim that UV-A and UV-B LEDs can detect UV-C light. Toole *et al.* 2009[39] claimed that using dual wavelengths increased the LED detector sensitivity and improved the detection limit by reducing baseline noise in post-column reaction systems.

3.2 Impact of environmental temperature

The impact of temperature is required to determine if thermal changes within the range of typical environmental temperature variations have a significant impact on the rLED monitored values. This is essential for the practical application of rLEDs in

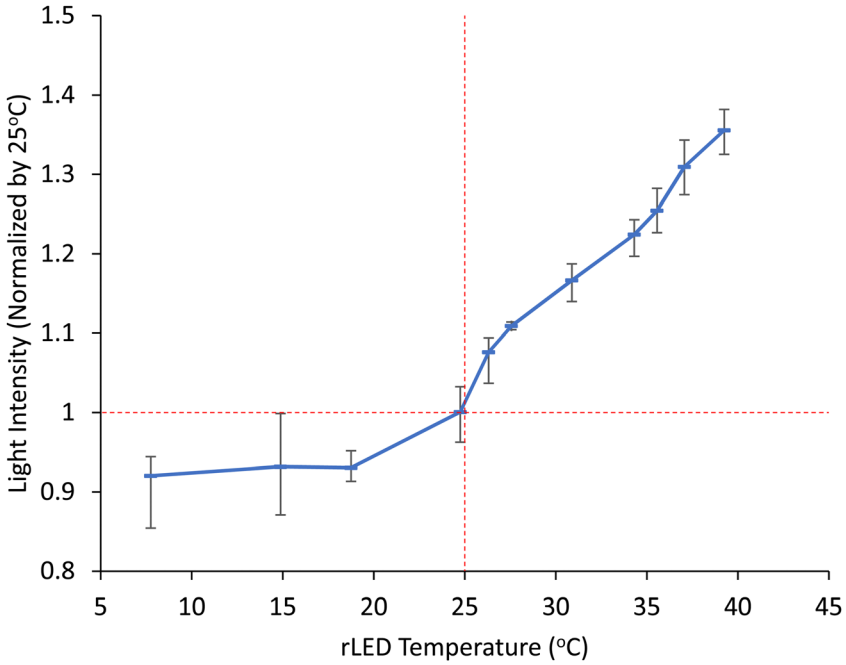

Fig. 5 365 nm/3 W rLED measurement dependency on temperature.

water disinfection systems. While the experimental method employed in this part did not yield quantitatively reliable results, it does offer valuable qualitative insights. As shown in Fig. 5, thermal changes within the range of typical environmental temperature variations have a significant impact on the rLED readings. The measurements show an approximate 8% drift when cooling down from room temperature; however, this drift increases significantly to nearly 35% when the temperature gets warmer. This substantial variation underscores the importance of accounting for temperature effects for accurate measurements.

Dasgupta *et al.* 1993[26] demonstrated that the optical output of the LED increased by a substantial range of 30% to 200% when the temperature decreased (using dry ice) while the baseline temperature remained at 22 °C, under the Vis LED operating at 560 nm. Dasgupta *et al.* 2003 stated that this temperature influence should be compensated for in LED-based sensor instruments,[37] and it is obvious that this temperature dependency is a critical factor that must be addressed to obtain accurate and valid intensity measurements. Subsequent research is required to determine the thermal effects on rLEDs' output. To overcome this challenge, it is recommended to integrate an environmental temperature sensor as part of the design. Additionally, a mathematical correction can be implemented to adjust the sensor's output for temperature-related variations, enhancing the accuracy and reliability of the measurements.

4. Conclusions

This study examined the use of reverse LEDs as UV-LED intensity detectors. The rLED concept meets the study requirements in terms of sensitivity, costs, availability, and physical dimensions. rLEDs exhibit several advantages over alternative methods, including system simplicity and proven feasibility in related technologies (such as absorption sensors), especially in light of significant advancements in LED quality over recent years, and the potential for sensor adaptability to future enhancements (such as simultaneous monitoring of multiple wavelengths and built-in thermal compensation). Across a broad range of source power levels, the rLED readings closely align with the values obtained from the calibrated spectroradiometer, even when employing low-cost LEDs. All measurements, except for the thermal effect assessments, were conducted in duplicates using two independent rLEDs to enhance reliability and accuracy. rLEDs characterized by the wavelength of 365 nm and 405 nm and power of 3 W and 1 W, respectively, showed accurate results (<1.5% difference from reference spectroradiometer and <2% standard deviation). One of the 3 W/365 nm rLEDs showed a 0.5% shift from the reference over all measured power ranges. The effectiveness of the rLED as an intensity detector depends on the rLED temperature and the rLED environment temperature.

In implementing solutions, and revisiting the initial problem, it becomes evident that in a "trade-off" system where quality or accuracy is weighed against costs or simplicity, a minor percentage of drift from the target values is acceptable. This is because the UV-LED water disinfection system can be designed to ensure that the UV dose applied to the water exceeds the minimum required dose by a considerable margin. By adhering to this design principle, the system can issue alerts for low-intensity levels even within a defined "safety band" thereby reducing the risk of contaminated water. However, the long-term stability of the rLEDs used as detectors under UV-C

irradiation should be intensively studied according to the UVC LED systems lifespan although the materials used in a UV-A LED show stability in this study. The most significant contribution of this work is the proof of the feasibility of utilizing standard LEDs in reverse mode as UV sensors with acceptable accuracy, particularly for water disinfection systems installed in low- and middle-income settings.

Author contributions

Dana Pousty: methodology, validation, formal analysis, investigation, writing – original draft. Yoav Gerchman: conceptualization, methodology, validation, formal analysis, investigation, writing – original draft. Hadas Mamane: resources, supervision, funding acquisition, writing – review & editing.

Data availability

The data supporting this article have been included as part of the ESI.†

Conflicts of interest

The authors declare that they have no known competing financial interests or personal relationships that could have appeared to influence the work reported in this paper.

Acknowledgements

This study was supported by the Asper Clean Water Fund, Canada–Israel and the Tel Aviv University Center for Combatting Pandemics (TCCP).

References

1 United Nations Children's Fund (UNICEF), World Health Organization (WHO). Progress on household drinking water, sanitation and hygiene 2000–2017 Special focus on inequalities, Launch version July 12 Main report Progress on Drinking Water, Sanitation and Hygiene, 2019, p. 140.
2 A. S. Narayan, S. J. Marks, R. Meierhofer, L. Strande, E. Tilley and C. Zurbrügg, *et al.*, Advancements in and integration of water, sanitation, and solid waste for low-and middle-income countries, *Annu. Rev. Environ. Resour.*, 2021, **46**, 193–219, DOI: **10.1146/annurev-environ-030620-**.
3 W. A. M. Hijnen, E. F. Beerendonk and G. J. Medema, Inactivation credit of UV radiation for viruses, bacteria and protozoan (oo)cysts in water: A review, *Water Res.*, 2006, **40**(1), 3–22.
4 C. Chatterley and K. Linden, Demonstration and evaluation of germicidal UV-LEDs for point-of-use water disinfection, *J. Water Health*, 2010, **8**(3), 479.
5 P. H. Quek and J. Hu, Indicators for photoreactivation and dark repair studies following ultraviolet disinfection, *J. Ind. Microbiol. Biotechnol.*, 2008, **35**(6), 533.
6 O. Autin, C. Romelot, L. Rust, J. Hart, P. Jarvis, J. MacAdam, S. A. Parsons and B. Jefferson, Evaluation of a UV-light emitting diodes unit for the removal of micropollutants in water for low energy advanced oxidation processes, *Chemosphere*, 2013, **92**, 745–751.
7 K. Song, M. Mohseni and F. Taghipour, Application of ultraviolet light-emitting diodes (UV-LEDs) for water disinfection: A review, *Water Res.*, 2016, **94**, 341–349, DOI: **10.1016/j.watres.2016.03.003**.
8 L. Gough Yumu, D. Roser, R. Corkish, A. Nicholas, P. Jagals and R. Stuetz, Photovoltaic powered ultraviolet and visible light-emitting diodes for sustainable point-of-use disinfection of drinking waters, *Sci. Total Environ.*, 2014, **493**, 185–196.
9 G. Y. Lui, D. Roser, R. Corkish, N. J. Ashbolt and R. Stuetz, Point-of-use water disinfection using ultraviolet and visible light-emitting diodes, *Sci. Total Environ.*, 2016, **553**, 626–635.
10 K. Oguma, R. Kita, H. Sakai, M. Murakami and S. Takizawa, Application of UV light emitting diodes to batch and flow-through water disinfection systems, *Desalination*, 2013, **328**, 24–30, DOI: **10.1016/j.desal.2013.08.014**.
11 D. Pousty, R. Hofmann, Y. Gerchman and H. Mamane, Wavelength-dependent time–dose reciprocity and stress mechanism for UV-LED disinfection of Escherichia coli, *J. Photochem. Photobiol., B*, 2021, **217**, 112129.
12 O. Lawal, J. Cosman and J. U. V.-C. Pagan, LED Devices and Systems: Current and Future State, *IUVA News*, 2018, **20**(1), 22–28.
13 R. Abbasinejad and D. Kacprzak, A comprehensive detailed formula for LED degradation and lifetime estimation leading to reduce CO_2 emissions, *Clean Eng. Technol.*, 2022, **9**, 100518.
14 C. Qian, X. J. Fan, J. J. Fan, C. A. Yuan and G. Q. Zhang, An accelerated test method of luminous flux depreciation for LED luminaires and lamps, *Reliab. Eng. Syst. Saf.*, 2016, **147**, 84–92.
15 W. Sun, M. Shatalov, J. Deng, X. Hu, J. Yang and A. Lunev, *et al.*, Efficiency droop in 245–247 nm AlGaN light-emitting diodes with continuous wave 2 mW output power, *Appl. Phys. Lett.*, 2010, **96**(6), 245–248.
16 D. Pousty, H. Mamane, V. Cohen-Yaniv and J. R. Bolton, Ultraviolet actinometry – Determination of the incident photon flux and quantum yields for photochemical systems using low-pressure and ultraviolet light-emitting diode light sources, *J. Environ. Chem. Eng.*, 2022, **10**, 107947.
17 H. J. Kuhn, S. E. Braslavsky and R. Schmidt, Chemical Actinometry, *Pure Appl. Chem.*, 2004, **76**(12), 1–47.
18 J. Rabani, H. Mamane, D. Pousty and J. R. Bolton, Invited Review Practical Chemical Actinometry; A Review, *Photochem. Photobiol.*, 2021, **97**, 873–902.
19 J. R. Bolton, M. I. Stefan, P. S. Shaw and K. R. Lykke, Determination of the quantum yields of the potassium ferrioxalate and potassium iodide-iodate actinometers and a method for the calibration of radiometer detectors, *J. Photochem. Photobiol., A*, 2011, **222**(1), 166–169, DOI: **10.1016/j.jphotochem.2011.05.017**.
20 J. R. Bolton, I. Mayor-Smith and K. G. Linden, Rethinking the Concepts of Fluence (UV Dose) and Fluence Rate: The Importance of Photon-based Units A Systemic Review, *Photochem. Photobiol.*, 2015, **91**(6), 1252–1262.

21 D. Pousty, H. Mamane, V. Cohen-Yaniv and J. R. Bolton, Protocol for UVC uridine actinometry Dana, *Methods J.*, 2023, **10**, 101957.
22 S. Goldstein and J. Rabani, Mechanism of Nitrite Formation by Nitrate Photolysis in Aqueous Solutions: The Role of Peroxynitrite, Nitrogen Dioxide, and Hydroxyl Radical Sara, *J. Am. Chem. Soc.*, 2007, **129**(34), 10597–10601.
23 K. G. Linden, N. Hull and V. Speight, Thinking Outside the Treatment Plant: UV for Water Distribution System Disinfection, *Acc. Chem. Res.*, 2019, **52**(5), 1226–1233.
24 P. Zarrintaj, H. Vahabi, M. Reza Saeb and M. Mozafari, Application of polyaniline and its derivatives, *Fundam. Emerging Appl. Polyaniline*, 2019, 259–272.
25 M. N. Khan, *Understanding LED Illumination*, CRC Press, 2013.
26 P. K. Dasgupta, H. S. Bellamy, H. Liu, J. L. Lopez, E. L. Loree and K. Morris, *et al.*, Light emitting diode based flow-through optical absorption detectors, *Talanta*, 1993, **4**(1), 53–74.
27 Ł. Tymecki and R. Koncki, Simplified paired-emitter-detector-diodes-based photometry with improved sensitivity, *Anal. Chim. Acta*, 2009, **639**(1–2), 73–77.
28 J. Kovac, L. Peternai and O. Lengyel, Advanced light emitting diodes structures for optoelectronic applications, *Thin Solid Films*, 2003, **433**(1–2), 22–26.
29 H. A. Flaschka, S. McClure and J. V. Hornstein, Determination of Manganese with Triethanolamine Using Long-Path Photometry, *Anal. Lett.*, 1978, **11**(5), 383–392.
30 O. M. Toole, K. T. Lau and D. Diamond, Photometric detection in flow analysis systems using integrated PEDDs, *Talanta*, 2005, **66**(5), 1340–1344.
31 M. O'Toole, K. T. Lau, R. Shepherd, C. Slater and D. Diamond, Determination of phosphate using a highly sensitive paired emitter–detector diode photometric flow detector, *Anal. Chim. Acta*, 2007, **597**, 290–294.
32 M. R. Riley, K. A. Jordan and M. L. Cox, Development of a cell-based sensing device to evaluate toxicity of inhaled materials Mark, *Biochem. Eng. J.*, 2004, 95–99.
33 M. O'Toole, K.-T. Lau, B. Shazmann, R. Shepherd, P. N. Nesterenko and B. Paull, *et al.*, Novel integrated paired emitter-detector diode (PEDD) as a miniaturized photometric detector in HPLC, *Soc. Chem.*, 2006, **131**, 938–943.
34 L. Barron, P. N. Nesterenko, D. Diamond, M. O'Toole, K. T. Lau and B. Paull, Low pressure ion chromatography with a low cost paired emitter–detector diode based detector for the determination of alkaline earth metals in water samp, *Anal. Chim. Acta*, 2006, **577**, 32–37.
35 K. T. Lau, W. S. Yerazunis, R. Shepherd and D. Diamond, Quantitative colorimetric analysis of dye mixtures using an optical photometer based on LED array, *Sens. Actuators, B.*, 2006, **114**, 819–825.
36 V. Lange, F. Lima and D. Kühlke, Multicolour LED in luminescence sensing application, *Sens. Actuators, A*, 2011, **169**, 43–48.
37 P. K. Dasgupta, I. Y. Eom, K. J. Morris and J. Li, Light emitting diode-based detectors: Absorbance, fluorescence and spectroelectrochemical measurements in a planar flow-through cell, *Anal. Chim. Acta*, 2003, **500**(1–2), 337–364.
38 M. O'Toole, D. D. Martina and D. Diamond., *Sensors*, 2008, **8**, 2453–2479.
39 O. M. Toole, L. Barron, R. Shepherd, B. Paull, P. Nesterenko and D. Diamond, Paired emitter–detector diode detection with dual wavelength monitoring for enhanced sensitivity to transition metals in ion chromatography with post-column reaction, *Anal*, 2009, **134**(1), 124–130.
40 F. J. Arques-Orobon, N. Nuñez, M. Vazquez, C. Segura-Antunez and V. González-Posadas, High-power UV-LED degradation: Continuous and cycled working condition influence, *Solid State Electron*, 2015, **111**, 111–117.